COOLING SYSTEMS FOR THE LU-10 ACCELERATING SECTION

V.F. Zhiglo, V.A. Kushnir, V.V. Mytrochenko, K.Yu. Kramarenko
National Science Center "Kharkov Institute of Physics and Technology", Kharkov, Ukraine
E-mail: zhiglo@kipt.kharkov.ua

Parameters and design of the cooling system of the accelerating section for industrial high power linac are given. It is shown that the heating of the outer surface of the accelerating section constitutes 1°C at average r.f.-power of 30 kW and cooling water flow of 80 l/min. Thermal deformations have little effect on the microwave-characteristics of the accelerating structure.

PACS: 29.20.Ej

INTRODUCTION

To increase the productivity of sterilization radiation technology of the medical products at the "Accelerator" R&D Production Establishment of NSC KIPT [1] and for carrying out scientific research it is necessary to raise the average beam power of the existing electron linac LU-10 [2]. Thus an upgrade of the LU-10 is needed.

The upgrade involves replacement of an obsolete r.f. source (KIU-12A klystron) with a commercially available r.f. source (VKS-8262F klystron). Because operating frequency of the new r.f. source that is 2.856 GHz is different from that of the old one the upgrade needs development and fabrication of a new accelerating section. The maximal average r.f. power of the new klystron is 36 kW. To provide reliable operation we plan to use just 30 kW of this power.

Operating temperature of the section was chosen equals to 40°C as some compromise between water cooling abilities at high ambient temperatures and the temperature limit of 50°C that is associated with the deposition of salts on the cooled surfaces that is significantly reduces the heat exchange. The increasing of the average power of the r.f. supply makes the great importance of estimation of the values of the probable thermal deformations of the section caused by its temperature inhomogeneity.

The calculation results of hydraulic and thermal regime of accelerating section designed for the LU-10 electron linac upgrading [3] are presented.

1. ACCELERATING SECTION DESIGN

Accelerating section (Fig. 1) consists of 87 resonance cells formed by brazed rings and discs and has a length of L_{ac} = 3 m [3]. R.F.-power supply is carried out through the waveguide *8* and the input coupler *1*. The output coupler 5 is used for deflation of r.f. power to the terminated load. The water supply is provided through fitting *11* and water drains through fitting *7*. After brazing in the vacuum furnace the accelerating section has to be placed into the solenoid [3]. The peculiarity of the technology consists in the fact that the output waveguide and fittings must be attached to the section after it's placing into the solenoid. Brazing by silver solder in the air is difficult, because the protection of copper accelerating structure and waveguides from oxidation is needed. To eliminate the brazing process, mounting of fittings *7, 11* and the output waveguide *8* can be made by welding in the air that does not require a protective atmosphere for the section. Two stainless steel inserts *9* and *10* are used for the connection of the output waveguide *8* to the coupler *5*. These inserts are brazed in a vacuum to the waveguide and coupler. Welding is performed on the junction of inserts.

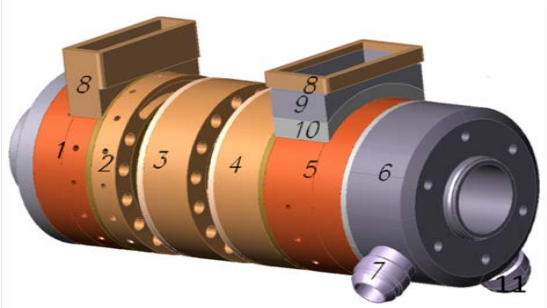

Fig. 1. Arrangement of the accelerating section LU-10, stainless steel is shown in gray color, the rest is copper

The cooling water enters from the inlet fitting *11*. Collector *6* distributes this water on cylindrical channels passing along the whole length of the section. The diameter of channels, which can be seen in rings in Fig. 1, is d = 8 mm.

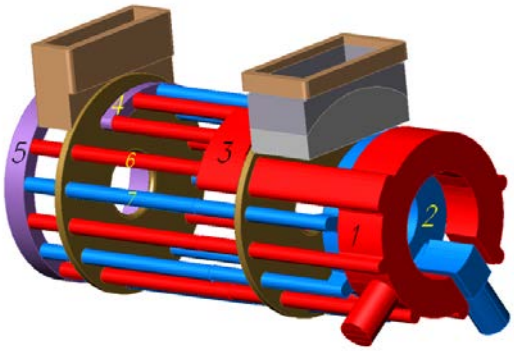

Fig. 2. Cooling channels and collectors of water input (blue) and water output (red)

Cooling channels and collectors filled with water are shown separately in Fig. 2. It can be seen that the back-loop heat exchange circuit is used. Camera *2* of the inlet collector distributes the stream on six channels going along whole section to the chamber *5* of input coupler, where the flow reverses back. Water output from the chamber *5* into the chamber *1* of outlet collector realizes by 6 channels (red). To cool the part of the section between input and output waveguides, additional loop *3*, *4* is also connected to cameras *1* and *2*. The outlet channels of this loop with an additional collector *3* are shown in red in Fig. 2. Supply and drain of water occurs here on two channels that connected in parallel. Change of the flow direction occurs in the chamber *4*.

Fig. 2 shows that the additional cooling loop (between the waveguides) violates azimuthal periodicity of cold and hot water channels. At significant heating this can cause the thermal deformations that violate the axial symmetry of the accelerating field. Using of stainless steel in the waveguide line is also the peculiarity of designed accelerating section. It may cause additional heating due to low electrical and thermal conductivity of this material relatively to copper.

2. CALCULATION METHOD

Taking into account the smallness of the expected temperatures in comparison with the temperatures of metal melting and water boiling, stationary homogeneous linear heat conduction problem is solved:

$$\lambda\vec{\nabla}\left(\vec{\nabla}T\right)=0,$$
$$\lambda\vec{n}\left(\vec{\nabla}T\right)\big|_s=q_s, \quad (1)$$

where λ is the thermal conductivity, T is the temperature, $\vec{n}$ is the normal vector to the boundary surface S, q_s is the heat flux density on S.

To solve the problem (1) in the case of axial symmetry, two dimensional codes can be used: $\lambda' = \lambda r$, $q'_s = q_s r$.

Thus, the slight change of absorbed r.f. power along the section allows to use the two dimensional approach for calculation of disks temperature in the region of output coupler and temperature of waveguide walls.

When the surface is heated by the r.f. field:

$$q_s = \frac{1}{2}R_s H_s^2, \quad (2)$$

where H_s is the magnetic field on the surface and R_s is the resistance of the skin depth (surface resistance).

$$R_s = \left(\pi\rho f \mu_0\right)^{1/2},$$

where ρ is the bulk resistance, f is the frequency of the r.f. field, μ_0 is the permeability constant.

For calculation of H_s the SUPERFISH code is used [4]. Disk loaded waveguide of the accelerating section LU-10 is a non-periodic traveling wave accelerating structure, so the direct use of the SUPERFISH code designed for standing wave structures is impossible. However, a special algorithm [5] allows evaluating such parameters of 2π/3 traveling wave structures as group velocity, wave attenuation and shunt impendence using field patterns in one and a half cells of the traveling-wave structure (Fig. 3). Knowing wave attenuation α_w for each cell of the section it is possible to obtain distribution of power losses $P(z)$ in the whole structure by solving equation:

$$dP(z)/dz = -2\alpha_w(z)P(z).$$

Longitudinal distribution of average rf-power losses in accelerating section without beam loading is shown in Fig. 4 for 30 kW of average input power. Cells are numbered from the input coupler. Number of the last cell (before output coupler) is № 87. Peaks of losses are located near the input and output couplers. It is obvious that these regions are of special interest for the calculation. The total power of losses is W = 10.7 kW.

Now to obtain H_s we use the square root of the sum of squares of magnetic field patterns on the surface of the one and a half cell (see Fig. 3) for two sets of boundary conditions. One of them corresponds to the cosine solution while another one corresponds to the sine solution of the 2π/3 travelling wave mode.

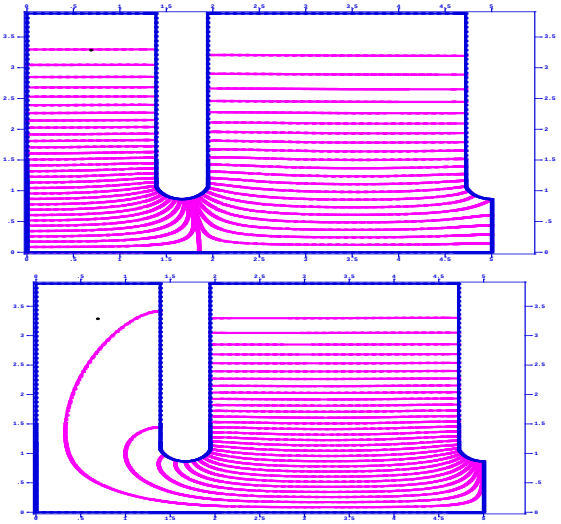

Fig. 3. Field distribution in the 1.5 cavity. The top pattern corresponds to the cosine solution while the bottom one corresponds to the sine solution of the 2π/3 travelling wave mode

Fields in the both cases is normalized by the same stored energy. Power dissipation needed to provide that stored energy is used to connect the cavity wall magnetic field with power losses (see Fig. 4).

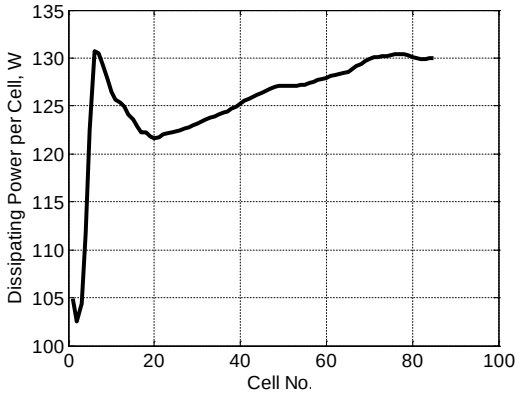

Fig. 4. Distribution of power losses per cell along the length of the accelerating structure

Simulated distribution of the magnetic field amplitude on the disk and ring surfaces of the last cell before the output coupler at an input r.f. power of 30 kW is shown in Fig. 5. Obtained data are substituted into Eq. (2).

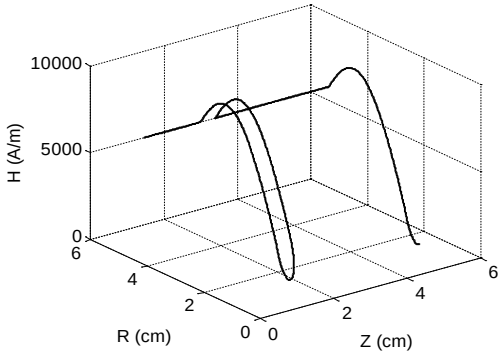

Fig. 5. Distribution of the magnetic field on the surface of the cell № 87

When the heat exchange takes place $q_s = \alpha(T_s - T_0)$, where α is the heat transfer coefficient, T_s is the temperature on the cooled surface S, T_0 is the water temperature on the axis of the cooling channel.

Coefficient α for water is calculated from empirical relationships for pipes with natural surface roughness [6], based on the water speed in the channel V and the flow regime.

By setting the heating of the cooling water on $\Delta T = 2°C$, from the condition of the heat balance between section and water one can obtain:

$$V = \frac{4W}{n\pi d^2 \rho C \Delta T}, \quad (3)$$

where n is the number of cooling channels, d is the channel diameter, ρ is the density and C is the specific heat of water, respectively.

Substituting the parameters of developed accelerating section in Eq.(3), one can obtain: $V = 3.3$ m/s and water flow $Q = n\pi d^2 V = 80$ l/min. Then we find the Reynolds number: $\mathrm{Re} = Vd/\nu = 4000$, where ν is the kinematic viscosity of water. Such value of the Reynolds number corresponds to turbulent flow regime for which the Nusselt number (the roughness of the channel walls is $\Delta = 10$ μ) equals to [6]:

$$Nu = 0.021 \cdot Re^{0.8} \cdot Pr^{0.43}, \quad (4)$$

where $Pr = 0.7$ is the Prandtl number for water.

Using the definition of Nu, we obtain a heat transfer coefficient: $\alpha = Nu \cdot k/d$, where k is the thermal conductivity of water. If rectangular cooling channels 1, 2, 3, 4, 5 (see Fig. 2) are used, Eq. (4) is also used by substituting a hydraulic diameter d_e instead of d: $d_e = 4s/p$, where s and p is an area and the perimeter of the channel cross section [6].

Upon cooling the outer surface of the accelerating section, such processes as thermal radiation (α_r) and free convection (α_c) [7] are taken into account. It is assumed that the temperature of surrounding walls and of the air is 20°C. In this case α depends on the temperature: $\alpha_r \sim T_s^3$, $\alpha_c \sim T_s^{0.25}/k(T)$. To avoid solving of nonlinear problem, the calculations made by iteration method of the stationary problem. Poor accuracy of this method has little effect on the accuracy of the final results, because of the smallness of α_r, and α_c relative to the heat transfer coefficient to the water α.

To solve the question about the feasibility of the selected cooling regime, the calculation of the water pressure drop in the system ΔP is required. It is known [8] that:

$$\Delta P = \sum_i \xi_i \frac{\rho V_i^2}{2} + \xi_{fr} \frac{\rho V^2}{2}, \quad (5)$$

where $\xi_{fr} = \lambda_{fr} L/d$, L is the length of the cooling channel, λ_{fr} is the equivalent coefficient of hydraulic friction, λ_i is the local hydraulic resistance coefficients, V_i is the local flow velocity.

3. CALCULATION RESULTS AND DISCUSSION

Substituting in Eq. (4) the thermal parameters of the water at 40°C, we find $\alpha = 1.5 \cdot 10^4$ W/(m^2·K). Then the difference between the average temperatures of the water and the section surface $T_s - T_0 = q_s/\alpha$ is obtained. Suppose that all the heat flow is passed through (allocated on) the cylindrical surfaces of 16 cooling channels: $W/(16 \cdot \pi \cdot d \cdot L_{ac} \cdot \alpha) = 0.3$°C. By setting the section average temperature of 40°C and the heating of the water on 2°C one can obtain the desired temperature of input water of 38.7°C. This parameter is important for the calculation of the operating regime of the cooling tower and the whole cooling system of the accelerator.

The hydraulic friction resistance between entrances in tubes in the rectangular ring of the collector may cause the additional difference in heating the water in adjacent channels. The maximum of this difference locates in the region of inlet of the water to the collector. Hydraulic calculations have shown that due to a short length of this part of the collector, the temperature deviation is < 0.05°C at temperature of input water of 39°C. Therefore the contribution of friction resistance is taken into account only for the cylindrical parts of the cooling channels.

In the back-loop system $L = 2L_{ac}$. Using the obtained value Re = 4000 with the roughness parameter of the walls of cooling channels $d/\Delta = 800$, according to graph [8], one can find $\lambda_{fr} = 0.03$, $\xi_{fr} = 22.5$. Presenting ΔP from Eq. (5) in the form of $\Delta P = \Delta P_l + \Delta P_{fr}$, we obtain the friction losses in the cylindrical cooling channel $\Delta P_{fr} = 1.217 \cdot 10^5$ Pa (1.2 at).

Local resistances are associated with the change of the direction or envelope of the flow. As can be seen from Fig. 2, such places correspond to: *a*) corner (bend) on the distributive (inlet) collector *2*; *b*) tee at the entrance into collector; *c*) collector; *d*) outlet of cooling tube into the chamber *5*. In the branch of reverse flow from the chamber *5* the following locations can be distinguished: *e*) entrance in the channel of backflow (red); f) collecting (outlet) collector; *g*) the transition to the tee fitting.

For simplicity we assume that the water passes only two collectors on eight channels. We consider that the collector in the additional cooling loop differs negligible. Each of the two annular collectors is presented in the form of two linear collectors of equivalent length. These linear collectors are connected in parallel. By calculating the local velocities V_i in according with the known cross sections and water flows, following [9], we obtain the pressure losses on the respective local resistances: $\Delta P_a = 7.3 \cdot 10^3$ Pa, $\Delta P_b = 1.6 \cdot 10^4$ Pa, $\Delta P_c = 7.17 \cdot 10^3$ Pa, $\Delta P_d = 5.4 \cdot 10^3$ Pa, $\Delta P_e = 2.7 \cdot 10^3$ Pa, $\Delta P_f = 1.1 \cdot 10^4$ Pa, $\Delta P_g = 2.7 \cdot 10^4$ Pa. The total local losses are $\Delta P_l = 7.67 \cdot 10^4$ Pa. The total losses of pressure in the cooling system are $\Delta P = 1.985 \cdot 10^5$ Pa (1.96 at). If the calculated value of the water flow is $Q = 80$ l/min and the pump efficiency is $\eta = 60\%$, one can obtain the minimum pump power $W_p = Q\Delta P/\eta = 444$ W. With regard to the necessary pressure at the inlet of the pump (depending on its type) and motor efficiency we have $W_p < 1$ kW.

The result of the calculation of the temperature corresponding to the magnetic field from Fig. 5 is shown in Fig. 6. The temperature drop on the disk radius is independent of the cooling. So this difference determines the limit of input r.f. power under the heat dissipation. As follows from Fig. 6, such drop is 2.5°C.

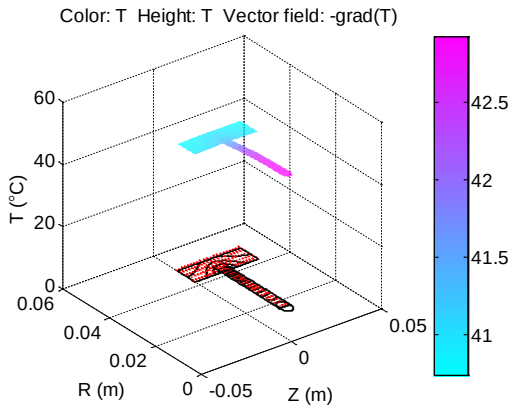

Fig. 6. Temperature distribution in cell No 87, top is the temperature, bottom is the isotherm

In used computational model the cylindrical cooling channels are located outside the boundary of the ring (are excluded from the calculation). At this the heat transfer coefficient α on the outer surface of the ring is taken equal to $1.5 \cdot 10^4$ Вт/(м^2·K), i.e. the same as in the cylindrical cooling channels (because the model is two-dimensional). As a result we obtain the small temperature gradient across the thickness of the ring. This confirms the permissibility of such approximation.

The temperature of the ring is little different from the temperature of the water. The temperature gradient in the ring is negligible.

At simulation of LU-10 accelerating section [3] with the PARMELA code [10] and [11], it was shown that the uniform heating of the section at 3°C through 5°C has no significant effect on its characteristics and beam dynamics. It is obvious that such conclusion is also valid in the case of uneven heating to the same temperature.

Thus the obtained results allow us to conclude that the designed cooling system will provide the operation of the accelerating section with the average r.f. power of 30 kW.

The insignificance of the temperature gradients in the ring of the cell, as mentioned above, allows to use two-dimensional models for investigating of the temperature azimuthal inhomogeneity.

Temperature distribution in the plane of the last disc No 87 of the section (before the output waveguide, which is shown on the right in Fig. 2) is shown in Fig. 7.

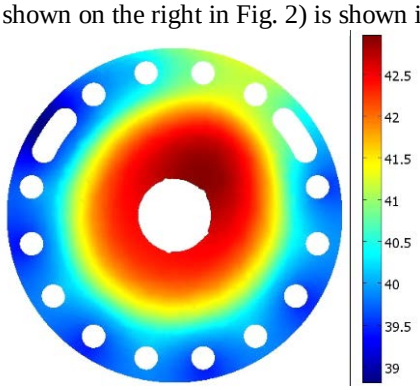

Fig. 7. Temperature distribution on the disk, window of water inlet channel is at the top left (the water is cold), window of water outlet channel is at the top right (the water is hot), circular holes on the perimeter are cylindrical cooling channels

The azimuthal asymmetry in the distribution is caused by the existence of windows of water inlet and outlet, as well as by the violation of the periodicity in the location of inlet and outlet channels (because of additional cooling loop, see comments in Sec.1). Peak of the temperature is shifted to the right, in the direction of the outlet window with heated water. The temperature difference of the water between the adjacent channels at the top of the disc equals 1°C. Nevertheless, it does not break significantly the homogeneity of the temperature distribution on disc in the region of periodical location of channels.

Hence the cooling channels do not cause significant asymmetry of the accelerating field. This result also confirms the permissibility of using a two-dimensional approach in solving the problem (the solution is illustrated in Fig. 6). The average heating of outer surface of the section is constant in the longitudinal direction that follows from the properties of the back-loop system. The value of the average heating constitutes about 1°C. The obtained value is of importance when the section is operating inside the solenoid.

To determine the temperature of inserts *9*, *10* (see Fig. 1), the plane problem of heat conduction for two contacting plates of stainless steel and copper is solved. Cooling of the steel plate corresponds to free convection. Cooling of the copper is carried out with a weak flow of water with α = 80 W/(m^2·K). The values of heat generation on the surfaces are taken from the reference literature on the rectangular waveguides (power dissipation in rectangular waveguides). Calculation is shown that, when the copper plate is cooled by free convection, the temperature of the steel plate is 71°C. When the copper plate is cooled by water, the temperature of the steel plate is 57°C. This shows the sufficiency of the thermal conductivity of stainless steel for reducing the temperature of inserts *9*, *10* by water cooled waveguide.

SUMMARY

Simulation is shown that developed cooling system provides the required characteristics of LU-10 accelerating section and its reliable operation. The heating of the outer surface of the accelerating section constitutes 1°C at average r.f. power of 30 kW and cooling water flow of 80 l/min. Thermal deformations have little effect on the r.f. characteristics of the accelerating structure. Power consumption needed to provide necessary coolant flow is less than 1 kW.

The work was partially performed under the contract K-9-29 NAS of Ukraine

REFERENCES

1. M.I. Aizatskyi, E.Z. Biller, A.N. Dovbnya, et al. Development accelerating sections for linear electron accelerators // *Problems of Atomic Science and Technology. Series "Nuclear Physics Investigations"*. 1999, № 1, p. 80-84.
2. V.I. Beloglazov, E.Z. Biller, V.A. Vishnyakov, et al. Industrial-Materials Science Accelerator Complex to Energies up to 10 MeV // *Problems of Atomic Science and Technology. Series "Radiation Damage Physics and Radiation Materials"*. 1986, № 1, p. 89-91.

3. M.I. Aizatskyi, A.N. Dovbnya, V.F. Zhiglo, et al. Accelerating System for an Industrial linac // *Problems of Atomic Science and Technology. Series "Nuclear Physics Investigations"*. 2012, № 4, p. 24-28.
4. J.H. Billen, L.M. Young. POISSON SUPERFISH on PC compatibles // *Proc. 1993 Particle Accelerator Conf.* Washington, USA. 1993, p. 790-792.
5. G.A. Loew, R.H. Miller, et al. // *IEEE Trans. Nucl. Sci.* 1979, v. NS-26, p. 3701.
6. M.A. Miheev, I.M. Miheeva. *Basis of Heat Transfer.* Moscow: «Energiya», 1977, p. 89-90.
7. H. Wong. *The Basic Formulas and Data on Heat Transfer for Engineers.* Moscow: «Atomizdat», 1979, p. 56-57, 89.
8. N.G. Lashutina, O.V. Makashova, et al. *The Technical Thermodynamics with Basis on the Heat Transfer and hydraulics.* Leningrad: «Mashinostroenie», 1988, p. 290 (in Russian).
9. I.E. Idelchic. *Handbook of hydraulic resistance.* Moscow: «Mashinostroenie». 1992, p. 257-401 (in Russian).
10. L.M. Young. PARMELA. Los Alamos, 1996 (preprint / Los Alamos National Laboratory, LA-UR-96-1835).
11. V.V. Mytrochenko, A. Opanasenko. Study of transient self-consistent beam dynamics in R.F. linacs using a particle tracing code // *NIM.* 2006, A 558, p. 235-239.

Article received 28.10.2015

СИСТЕМА ОХЛАЖДЕНИЯ УСКОРЯЮЩЕЙ СЕКЦИИ ЛУ-10

В.Ф. Жигло, В.А. Кушнир, В.В. Митроченко, К.Ю. Крамаренко

Приведены параметры и конструкция системы охлаждения ускоряющей секции для промышленного мощного линейного ускорителя. Показано, что нагрев внешней поверхности ускоряющей секции составляет 1°С при средней СВЧ-мощности 30 кВт и потоке охлаждающей воды 80 л/мин. Тепловые деформации оказывают несущественное влияние на СВЧ-характеристики ускоряющей структуры.

СИСТЕМА ОХОЛОДЖЕННЯ ПРИСКОРЮЮЧОЇ СЕКЦІЇ ЛУ-10

В.Ф. Жигло, В.А. Кушнір, В.В. Митроченко, К.Ю. Крамаренко

Наведено параметри і конструкцію системи охолодження прискорюючої секції для промислового потужного лінійного прискорювача. Показано, що нагрів зовнішньої поверхні прискорюючої секції становить 1°С при середній НВЧ-потужності 30 кВт і потоці охолоджуючої води 80 л/хв. Теплові деформації несуттєво впливають на НВЧ-характеристики прискорюючої структури.